Applied and Environmental Microbiology

Physiology and Metabolism | Full-Length Text

The catabolism of lignin-derived *p*-methoxylated aromatic compounds by *Rhodococcus jostii* RHA1

Megan E. Wolf,[1] Anne T. Lalande,[1] Brianne L. Newman,[1] Alissa C. Bleem,[2] Chad T. Palumbo,[2] Gregg T. Beckham,[2] Lindsay D. Eltis[1]

AUTHOR AFFILIATIONS See affiliation list on p. 15.

ABSTRACT Emergent strategies to valorize lignin, an abundant but underutilized aromatic biopolymer, include tandem processes that integrate chemical depolymerization and biological catalysis. To date, aromatic monomers from C–O bond cleavage of lignin have been converted to bioproducts, but the presence of recalcitrant C–C bonds in lignin limits the product yield. A promising chemocatalytic strategy that overcomes this limitation involves phenol methyl protection and autoxidation. Incorporating this into a tandem process requires microbial cell factories able to transform the *p*-methoxylated products in the resulting methylated lignin stream. In this study, we assessed the ability of *Rhodococcus jostii* RHA1 to catabolize the major aromatic products in a methylated lignin stream and elucidated the pathways responsible for this catabolism. RHA1 grew on a methylated pine lignin stream, catabolizing the major aromatic monomers: *p*-methoxybenzoate (*p*-MBA), veratrate, and veratraldehyde. Bioinformatic analyses suggested that a cytochrome P450, PbdA, and its cognate reductase, PbdB, are involved in *p*-MBA catabolism. Gene deletion studies established that both *pbdA* and *pbdB* are essential for growth on *p*-MBA and several derivatives. Furthermore, a deletion mutant of a candidate *p*-hydroxybenzoate (*p*-HBA) hydroxylase, Δ*pobA*, did not grow on *p*-HBA. Veratraldehyde and veratrate catabolism required both vanillin dehydrogenase (Vdh) and vanillate *O*-demethylase (VanAB), revealing previously unknown roles of these enzymes. Finally, a Δ*pcaL* strain grew on neither *p*-MBA nor veratrate, indicating they are catabolized through the β-ketoadipate pathway. This study expands our understanding of the bacterial catabolism of aromatic compounds and facilitates the development of biocatalysts for lignin valorization.

IMPORTANCE Lignin, an abundant aromatic polymer found in plant biomass, is a promising renewable replacement for fossil fuels as a feedstock for the chemical industry. Strategies for upgrading lignin include processes that couple the catalytic fractionation of biomass and biocatalytic transformation of the resulting aromatic compounds with a microbial cell factory. Engineering microbial cell factories for this biocatalysis requires characterization of bacterial pathways involved in catabolizing lignin-derived aromatic compounds. This study identifies new pathways for lignin-derived aromatic degradation in *Rhodococcus*, a genus of bacteria well suited for biocatalysis. Additionally, we describe previously unknown activities of characterized enzymes on lignin-derived compounds, expanding their utility. This work advances the development of strategies to replace fossil fuel-based feedstocks with sustainable alternatives.

KEYWORDS metabolism, lignin, aromatic compounds, physiology, environmental microbiology, biocatalysis

Lignin is an abundant biopolymer in the cell walls of vascular plants, where its hydrophobic, aromatic moieties linked by C–C and C–O bonds support and protect plant tissues. This critical polymer comprises up to 30% of biomass and 30% of organic

Editor Arpita Bose, Washington University in St. Louis, St. Louis, Missouri, USA

Address correspondence to Lindsay D. Eltis, leltis@mail.ubc.ca.

The authors declare no conflict of interest.

See the funding table on p. 15.

Received 30 November 2023
Accepted 23 January 2024
Published 21 February 2024

carbon on earth (1). In plants, lignin is synthesized by radical coupling of phenolics, including hydroxycinnamyl acid derivatives, most of which have at least one methoxy substituent (2). The polymer is therefore complex, irregular, and highly methoxylated (Fig. 1A). Due to its abundance, lignin is an attractive, renewable feedstock to displace fossil fuels for the sustainable manufacturing of chemicals such as dicarboxylic acids, lipids, and aromatics (3). However, its heterogeneity, reactivity, and association with plant polysaccharides present significant barriers to its valorization. The use of tandem processes that integrate chemical and biological catalysis has emerged as a promising strategy for lignin valorization (4–6). In these processes, thermochemical fractionation of the biomass yields a mixture of lignin-derived aromatic compounds (LDACs), which is then transformed by a microbial cell factory into a single, target compound. Biocatalysis exploits the naturally convergent nature of aromatic catabolism in bacteria (6). However, efficient production of the target compound requires that the biocatalyst be tuned to the mixture of LDACs, whose composition depends on the biomass and the chemo-catalytic depolymerization process (4).

A variety of methods have been developed for depolymerizing lignin, the majority of which primarily cleave the C–O linkages (3, 15–17). For example, reductive catalytic

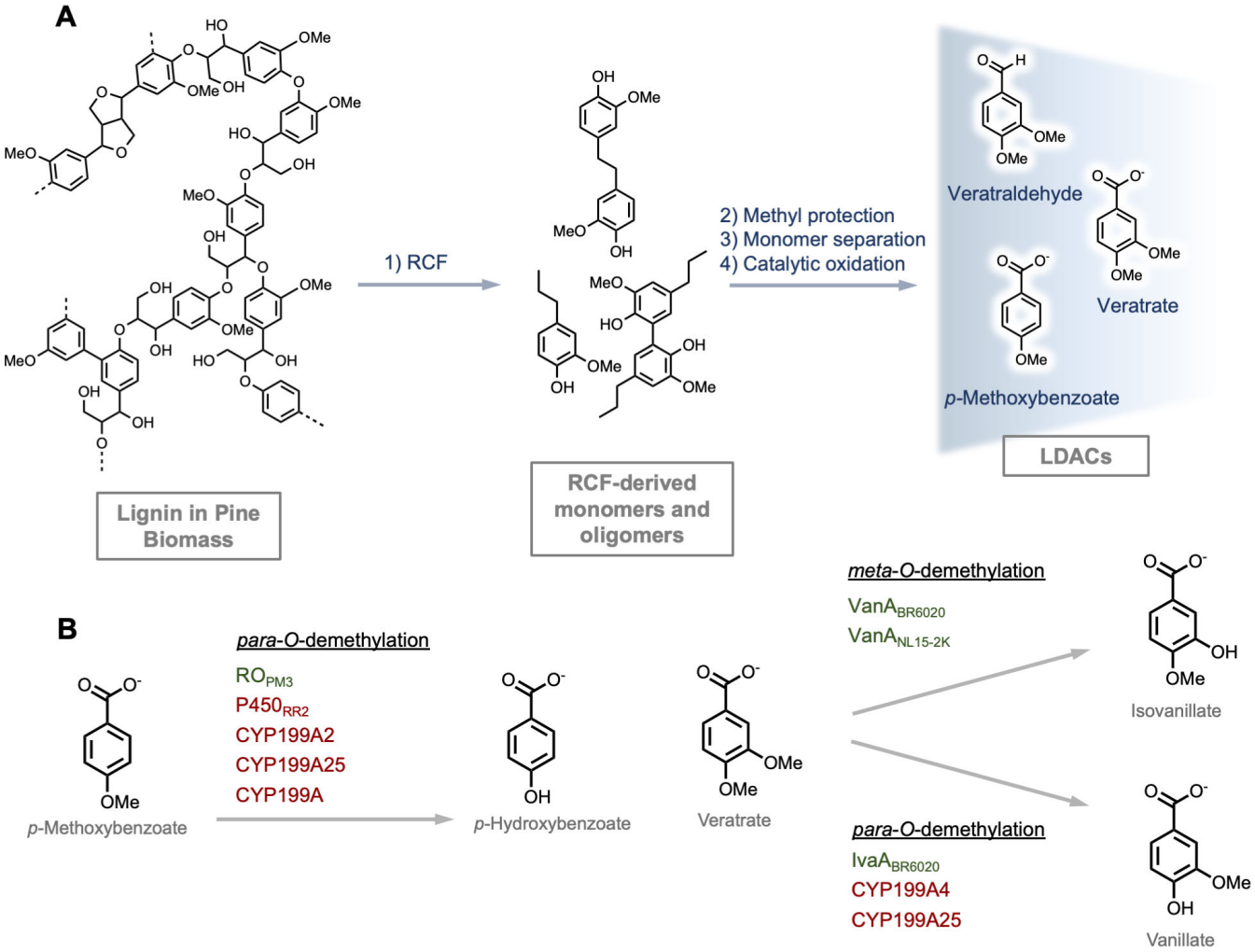

FIG 1 (A) Summary of the chemocatalytic fractionation of pine biomass to veratrate, *p*-MBA, and veratraldehyde as described in Palumbo et al. (7). (B) ROs (green) are RO_{PM3} from *Pseudomonas* PM3 (8), $VanA_{BR6020}$ from *Comamonas testosteroni* BR6020 (9), $VanA_{NL\ 15\text{-}2K}$ from *Streptomyces* sp. NL 15–2K (10), and $IvaA_{BR6020}$ from *C. testosteroni* BR6020 (9). P450s (red) are $P450_{RR2}$ from *Rhodococcus rhodochrous* strain 116 (11), CYP199A2 (12), CYP199A25 (13), and CYP199A4 (14). For clarity, only aromatic substrates and products are displayed. In all shown enzymatic reactions, one equivalent of NADH, H^+, and molecular oxygen are consumed per aromatic substrate, and one equivalent of NAD^+, water, and formaldehyde are produced per aromatic product.

fractionation (RCF) cleaves the C–O bonds in lignin to near theoretical yields (18). Unfortunately, the C–C linkages are recalcitrant to RCF and many other methods (19), leaving many lignin aromatics inaccessible in dimeric and oligomeric structures. To overcome this limitation, emerging chemo-catalytic strategies target C–C linkages with oxidation (20, 21). As one example, Palumbo et al. recently reported C–C bond cleavage catalysis of the dimers and oligomers in pine RCF lignin oil through radical autoxidation, in a process that requires the protection of the phenol groups due to their antioxidant nature. Phenol protection by methylation enabled autoxidation with a Mn/Zr catalyst system, yielding a lignin stream enriched in the monomeric compounds veratrate, veratraldehyde, and *p*-methoxybenzoate (*p*-MBA) (Fig. 1B) (7). As the major LDACs in this lignin stream are *p*-methylated, the discovery and characterization of *p*-*O*-demethylation pathways and enzymes are imperative for developing effective biocatalysts. Indeed, metabolic engineering has revealed that *O*-demethylation is a potentially rate-limiting step in the biocatalytic transformation of LDACs (22), and *p*-*O*-demethylation pathways are not native to some of the strains being developed as microbial cell factories, such as *Pseudomonas putida* KT2440 (7).

Rieske-type oxygenases (ROs) and cytochromes P450 (P450s) are two families of enzymes that are widespread in bacteria and that catalyze the *O*-demethylation of LDACs (22). ROs and P450s utilize a mononuclear iron or heme prosthetic group, respectively, to activate dioxygen for the *O*-demethylation reaction. Both the RO- and P450-catalyzed reactions require two reducing equivalents, typically originating from NAD(P)H, and result in the production of water and formaldehyde. Electron transfer from NAD(P)H to the oxygenase is mediated by a flavin-containing reductase through a ferredoxin domain, which can either be linked to the reductase domain or can occur as a separate component (23). The architecture of these reductases varies. For example, the respective reductases of the phthalate dioxygenase (24) and vanillate *O*-demethylase (25) systems are characterized by an N-terminal flavin-containing domain and a C-terminal 2Fe-2S-containing domain. Interestingly, homologous "phthalate dioxygenase reductase" (PDR)-type components have been reported as part of two-component P450-reductase systems (26). Among ROs and P450s catalyzing *O*-demethylation, several have been reported to act on *p*-methoxylated LDACs (Fig. 1B). For example, ROs catalyze the *p*-*O*-demethylation of *p*-MBA and veratrate in pseudomonads and *Comamonas testosteroni*, respectively (8, 9). Similarly, $P450_{RR2}$ was induced in *Rhodococcus rhodochrous* strain 116 by growth on *p*-MBA and *p*-ethoxybenzoate (11). $P450_{RR2}$ bound *p*-MBA tightly, suggesting the enzyme catalyzes the *O*-demethylation of this compound. More recently, several members of the P450 subfamily CYP199A were shown to selectively *p*-*O*-demethylate *p*-MBA and veratrate although the subsequent catabolism of these compounds was not fully elucidated (12–14). However, the CYP199A4 system from *Rhodopseudomonas palustris* has been expressed in engineered strains of *P. putida* KT2440 for catabolism of *p*-methoxylated LDACs from RCF (7).

Rhodococcus is a genus of bacteria that catabolizes an exceptionally wide range of aromatic compounds (27, 28). Growth substrates include alkylguaiacols and acetovanillone, which are derived from the chemocatalytic fractionation of diverse biomass feedstocks (7, 29–32). Their catabolic capacity, combined with their high resistance to stressors such as organic solvents, contribute to rhodococci being ideal candidates for biocatalysis (33), and indeed, rhodococcal biocatalysts are used to generate thousands of tons of acrylamide annually (34). The engineering and optimization of rhodococcal biocatalysts are further assisted by the availability of numerous genetic tools (35–37). Within this genus, *Rhodococcus jostii* RHA1 (RHA1 hereafter), originally isolated from lindane-contaminated soil, has been well characterized for its ability to catabolize a variety of aromatic compounds and steroids (38, 39). Relevant to this study, RHA1's ability to catabolize veratraldehyde and veratrate has not been investigated. However, the catabolism of their *p*-*O*-demethylated counterparts, vanillin and vanillate, respectively, have been described (40). Briefly, a vanillin dehydrogenase, Vdh, catalyzes the oxidation of vanillin to vanillate, and the two-component RO, VanAB, catalyzes the

O-demethylation of vanillate to protocatechuate. Protocatechuate is catabolized to central metabolites via the β-ketoadipate pathway, which is encoded by the *pca* genes (41, 42). Indeed, although several bacterial strains have been reported to grow on veratraldehyde (43, 44), the genetic basis for this catabolism has yet to be validated.

In this study, we evaluated the potential of RHA1 as a biocatalyst for the valorization of methylated lignin streams. To do this, we first tested the ability of RHA1 to utilize a methylated lignin stream as a growth substrate. We then elucidated the catabolic pathway of each of the major *p*-methoxylated aromatic monomers in the mixture: veratraldehyde, veratrate, and *p*-MBA. Catabolic pathways were elucidated by growth analysis of deletion mutants and investigating metabolite accumulation. These mutants included the previously constructed Δ*vdh*, Δ*vanA* (40), and Δ*pcaL* (42) deletion mutants due to the chemical similarity of veratraldehyde and veratrate with vanillin and vanillate, respectively. The results are discussed with respect to establishing RHA1 as a viable biocatalyst to transform methylated lignin streams and, more generally, to the engineering and development of application-specific microbial cell factories for valorizing lignin.

MATERIALS AND METHODS

Chemicals and reagents

All reagents were of analytical grade unless otherwise noted. Reagents were obtained from Sigma-Aldrich and Fisher Scientific. Media were prepared using water purified on a Barnstead NANOpure UV apparatus to a resistivity of greater than 16 MΩ/cm.

Preparation of methylated pine RCF oligomers

Loblolly pine woodchips were subject to RCF as described previously (45). The resultant oil was methylated by stirring with excess methyl iodide and potassium carbonate in acetonitrile. Following workup, the methylated pine RCF oil was separated into two fractions by vacuum distillation, affording an oil distillate and a solid oligomeric substrate that remained in the stirred and heated flask. The solid was dissolved in ethyl acetate and filtered, and the volatiles were removed by rotary evaporation affording methylated pine RCF oligomers as a brown solid.

Oxidation of methylated pine RCF oligomers

Methylated lignin oligomers were oxidized as described previously (7). Briefly, 75 mL Parr batch reactor fit with a glass liner insert was charged with 65 mg of methylated pine RCF oligomers, acetic acid (15 mL), a stir bar, and $Mn(OAc)_2{\cdot}4H_2O$ (5.2 mg) and Zr(acetylacetonate)$_4$ (7.8 mg) catalyst. The mixture was pressurized three times with pure nitrogen and subsequently charged with air (29 bar) and dinitrogen (31 bar), achieving 6 bar total pressure of O_2 diluted to 10%. The vessel was heated to 150°C. Once at temperature, it was left to react for 1.5 h and subsequently cooled in an ice bath. Aliquots of 10–12 mL were taken from the reactions, and the acetic acid was removed under a stream of nitrogen, leaving an oil residue, which was used as a growth substrate. Gas chromatography-flame ionization detection (GC-FID) quantification of the monomers in the two different preparations is shown in Fig. S8.

Growth of bacterial strains

RHA1 was grown in M9 medium supplemented with goodies (M9G) (46) and the indicated carbon substrate for 2 days shaking at 30°C. Growth substrates were solubilized in dimethyl sulfoxide (DMSO) and added to media at appropriate concentrations. The pellet was then harvested and washed twice with M9G and added to M9G containing the experimental carbon substrate unless otherwise indicated. For the Δ*pbdA* and Δ*pcaL* growth experiment, cells were precultured in 10 mM benzoate and grown in 150 µL media in a round-bottomed 96-well (Corning) plate shaking continuously in a

Tecan Spark microplate reader. For growth on the methylated lignin stream, cells were grown in 5 mM veratrate, and 10-mL cultures were grown in 50 mL flasks. optical density (OD_{600}) was measured using a Cary 60 spectrophotometer. The methylated lignin substrate was introduced into M9G at a concentration of 10% vol/vol. Briefly, the methylated lignin product was treated with NaOH to precipitate the metal catalyst and neutralized with HCl. The substrate was filtered to remove particulate matter and sterilized prior to addition into growth media. For the wild-type (WT) growth experiment on veratraldehyde, cells were precultured in 3 mM veratraldehyde and grown in 25 mL M9G containing 3 mM veratraldehyde in 125-mL flasks. OD_{600} was measured using a Biochrom WPA Biowave II UV/visible spectrophotometer. For the Δ*pbdA* and Δ*vanA* intermediate accumulation experiment, cells were precultured in 5 mM benzoate and then grown in 25 mL of M9G containing 1 mM benzoate until the cultures had no significant change in OD_{600} (stationary phase), and veratrate was then added to 0.8 mM. OD_{600} was measured using a Biochrom WPA Biowave II UV/visible spectrophotometer. For the Δ*vdh* experiment, the mutant was precultured in 1 mM benzaldehyde while WT and the complement were precultured in 1 mM veratraldehyde. Cells were then grown in 500 µL M9G containing 3 mM veratraldehyde in a 48-well plate shaking continuously at 30°C. OD_{600} was measured using a Tecan Infinite M200 microplate reader. For the Δ*pbdB* and Δ*pobA* experiments, cells were precultured in 5 mM benzoate and grown in 500 µL M9G containing 5 mM *p*-MBA and *p*-HBA, respectively, in a 48-well plate. OD_{600} was measured using a Tecan Infinite M200 plate reader. CFU/mL was measured by plating dilutions of cell cultures in saline on lysogeny broth (LB) agar plates, and counting colonies after incubation for 2 d at 30°C.

LC/MS analyses

Liquid chromatography-mass spectrometry (LC-MS) analyses were performed using an Agilent 1290 Infinity II UHPLC in line with an Agilent 6546 Q-TOF equipped with a dual AJS ESI source operating in positive ionization mode. A sample (2 µL) was injected onto a Zorbax Eclipse Plus C18 Rapid Resolution HD, 2.1 × 100 mm 1.8 µm column and run on a 20 min linear gradient from 5% to 100% solvent B at 0.45 mL min^{-1}. Solvent A was 0.1% formic acid in water, and solvent B was 0.1% formic acid in methanol. MS parameters were as follows: capillary voltage, 3,500 V; nozzle voltage, 500 V; drying gas temp, 300°C; drying gas flow rate, 10 L min^{-1}; sheath gas temperature, 350°C; sheath gas flow rate, 12 L min^{-1}; nebulizer pressure, 45 psi; fragmentor voltage, 100 V. Data were collected using MassHunter Workstation LC/MS Data Acquisition version 10.1 and analyzed using MassHunter Workstation Qualitative Analysis version 10.0. Concentrations were determined by interpolation on a standard curve of 0–200 µM.

GC analyses

GC-FID analyses were performed using an Agilent Technologies 8890 autosampler. GC-MS analyses were performed using an Agilent Technologies 7890A autosampler equipped with a 5975C inert XL MSD with a Triple-Axis Detector. The GC-MS was operated with the same temperatures, injection volumes, and programmed temperature ramps as those used for GC-FID (see below) to enable comparable retention times. A 1-µL injection was used with a split ratio of 10:1. A 30 m × 250 µm × 0.25 µm Agilent Technologies HP-5ms column was used. The inlet temperature was set to 260°C. The oven was initially held at 50°C for 2 min and then ramped at 40°C min^{-1} until 100°C. The ramp was then changed to 5°C min^{-1} until 110°C where it was held for 5 min. The method continued to ramp at 5°C min^{-1} until 160°C where the temperature was held for 2 min. The temperature was then ramped at 25°C min^{-1} until 300°C where it was held for 2 min, reaching a total duration of 29.85 min. A flame ionization detector was used to quantify the products, and calibration curves were generated for the oxidation products based on peak area ratios between analyte standards and a naphthalene internal standard. The analyte mixture was obtained as described previously (7).

Gene deletion and DNA manipulation

Plasmids and primers used in this study are listed in Table S1 and S2, respectively. DNA was propagated, purified, and manipulated using standard procedures (47). The *pbdA*, *pbdB*, and *pobA* genes were deleted using *sacB* counterselection as described previously (48) to generate the Δ*pbdA*, Δ*pbdB*, and Δ*pobA* strains, respectively (Table 1). Flanking regions were amplified using the primers in Table S2 and inserted into p18mobsacB using Gibson assembly. The plasmid was conjugated into RHA1, and mutagenesis was performed by selecting for two successive crossover events. The candidate mutants were screened using colony PCR and screening primers in Table S2 (Fig. S3B). The *pbdB* and *pbdA* complementation plasmids were constructed via Gibson assembly using PCR amplicons generated using appropriate primers (Table S2) and linearized pTipQC1 plasmid. The *vdh* and *pobA* complementation plasmids were similarly constructed via Gibson assembly using linearized pRIME vector (49). *Escherichia coli* DH5α was used for all plasmid propagation and storage.

HPLC analysis

For detection of aromatic monomers, culture supernatants were acidified by adding acetic acid to 10% final concentration, centrifuged (16,000×*g* for 10 min), and filtered through a 0.2 µm polytetrafluoroethylene (PTFE) membrane. Samples were run over a Luna 5 µm C18 (2) 100 Å 150 × 3 mm column (Phenomenex) at 0.7 mL min^{-1} by a Waters 2695 separation high-performance liquid chromatography (HPLC) module. The samples were eluted with a 16.8 mL linear gradient from 1% methanol plus 0.1% formic acid in water to 100% methanol plus 0.1% formic acid and were monitored at 280 nm with a Waters 2996 photodiode array detector. Concentrations were determined by interpolation on a standard curve of 0 to 3 mM of authentic standard. For acetate quantification, culture supernatants were acidified by adding sulfuric acid to 20% final concentration and centrifuged (16,000×*g* for 10 min). Samples were run over an Aminex HPX-87H 250 × 4 mm column at 0.6 mL min^{-1} at 35°C using a Waters 2695 separation HPLC module with an isocratic 8 mM sulfuric acid mobile phase. Acetate was detected at 210 nm with a Waters 2996 photodiode array detector. Concentrations were determined by interpolation on a calibration curve of 0 to 30 mM of authentic standard.

RESULTS

Growth of RHA1 on a methylated lignin stream and consumption of components

To investigate the ability of RHA1 to transform a lignin stream derived from autoxidative C–C cleavage of methylated pine RCF oligomers, we first evaluated the growth of the strain on minimal media supplemented with this substrate at a 10% vol/vol concentration. Under these conditions, RHA1 grew robustly as measured by OD_{600} (Fig. 2; Fig. S1) and CFU (Fig. S2A and B). The results were replicated with two separately oxidized lignin substrates that contained final concentrations in the growth media of up to 400 µM veratrate, 68 µM veratraldehyde, and 19 µM *p*-MBA (Table 2). Acetate, derived from the acetic acid solvent of the autoxidation step, was present at up to 10 mM. To

TABLE 1 *Rhodococcus jostii* strains used in this study

Strain	Description	Source
RHA1	Wild-type *R. jostii* RHA1	(39)
Δ*pbdA*	RHA1 *pbdA* knockout	This study
Δ*pbdB*	RHA1 *pbdB* knockout	This study
Δ*pobA*	RHA1 *pobA* knockout	This study
Δ*vdh*	RHA1 *vdh* knockout	(40)
Δ*vanA*	RHA1 *vanA* knockout	(40)
Δ*pcaL*	RHA1 *pcaL* knockout	(42)

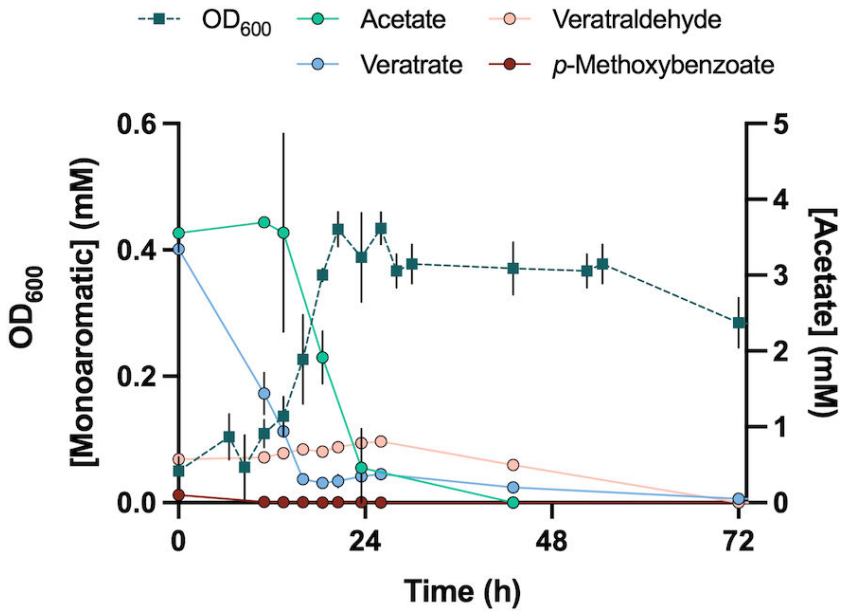

FIG 2 Growth of RHA1 on methylated lignin stream and consumption of major components. Aromatic monomers (left axis) and acetate (right axis) were monitored by HPLC. Cultures were grown in flasks on minimal medium supplemented with 10% Preparation A (Table 1; Fig. S8) at 30°C. Data are for one representative preparation and represent the mean of biological triplicates. Error bars represent the standard deviation.

determine whether RHA1 catabolized the components of the methylated lignin stream, we measured the concentration of constituent compounds during growth. As shown in Figure 2, RHA1 consumed all of the veratrate, veratraldehyde, *p*-MBA, and acetate within 96 h of inoculation. Although growth was monophasic, consumption of compounds was successive and overlapping. The aromatic acids veratrate and *p*-MBA were consumed first, followed by acetate and, lastly, veratraldehyde.

Identification of *pbdAB*

As RHA1 efficiently catabolized the *p*-methoxylated benzoates, *p*-MBA, and veratrate, in the methylated lignin stream, we interrogated the genetic determinants of the catabolic pathway. Of particular interest was the *p*-*O*-demethylation step, which is essential for further catabolism and for which no enzymes have previously been identified in RHA1 to our knowledge. As several P450s catalyze the *O*-demethylation of LDACs (41, 50), we searched the P450 contingent of RHA1 for candidate enzymes. The RHA1 gene RS14355 encodes a P450 in the CYP199A subfamily, designated CYP199A3. CYP199A3 shares at least 53% amino acid sequence identity with the other members of the subfamily and shares the highest sequence identity with CYP199A25 (74%) (Table 2) (12–14, 51). As CYP199A25 catalyzes the *O*-demethylation of *p*-substituted benzoates, we hypothesized that the P450 encoded by RS14355, annotated here as *pbdA*, exhibits a similar function. RS14360, annotated as *pbdB*, is located immediately upstream of *pbdA* in a putative operon (Fig. S3A) and encodes a predicted PDR-type reductase (Table 3). The putative

TABLE 2 Concentrations of aromatic monomers and acetate in the growth media containing 10% methylated lignin preparations

Substrate	Preparation A, µM	Preparation B, µM
Veratraldehyde	68 (6)	7 (2)
Veratrate	400 (40)	390 (10)
p-Methoxybenzoate	12.3 (0.8)	19 (5)
Acetate	3,500 (300)	9,800 (300)

operon also includes RS14365 directly upstream of *pbdB*. RS14365 encodes a TetR/AcrR family transcriptional regulator and was therefore annotated as *pbdR* (Table 3) (52).

Growth phenotype of the Δ*pbdA* and Δ*pbdB* deletion strains

To determine the role of *pbdAB* in the catabolism of *p*-MBA and veratrate, we constructed deletion mutant strains of each gene and evaluated their growth on these compounds. The Δ*pbdA* strain did not grow on *p*-MBA or veratrate (Fig. 3A and C), but grew as WT RHA1 on the *O*-demethylated products, *p*-HBA and vanillate, respectively (Fig. 3B and D). There was a small increase in OD_{600} when we tested the growth of the Δ*pbdA* strain on *p*-MBA and *p*-HBA (Fig. 3A and B). However, endpoint CFU/mL excluded the possibility that this represented genuine growth (Fig. S4). A complement strain harboring the pTip plasmid expressing *pbdA* fully rescued wild-type growth on *p*-MBA and veratrate (Fig. 3A and C). Similarly, the Δ*pbdB* strain did not grow on *p*-MBA (Fig. 4), but grew on benzoate (Fig. S5), which is metabolized through the catechol branch of the β-ketoadipate pathway. The wild-type phenotype was rescued by complementing the Δ*pbdB* strain with the pTip plasmid expressing *pbdB*. Together, these results indicate that both PbdA and PbdB are necessary for *p*-MBA catabolism. Moreover, Δ*pbdA* grew robustly on *p*-HBA and vanillate, the *p*-*O*-demethylated counterparts of *p*-MBA and veratrate, consistent with PbdAB catalyzing *O*-demethylation specifically at the *para* position.

Growth phenotype of the Δ*pcaL* deletion strain

To determine how *p*-MBA and veratrate are further catabolized to central metabolites, we tested the ability of the previously constructed Δ*pcaL* mutant to grow on *p*-MBA and veratrate, as well as their *p*-*O*-demethylated counterparts, *p*-HBA and vanillate. PcaL is a key enzyme in the β-ketoadipate pathway where it functions both as a γ-carboxymuconolactone decarboxylase and β-ketoadipate enol-lactone hydrolase, and is the point of convergence of the protocatechuate and catechol arms of the pathway (Fig. S6B) (42). As expected, the Δ*pcaL* mutant did not grow on any of the four tested aromatic substrates, but grew robustly on acetate, which is not metabolized through the β-ketoadipate pathway (Fig. S6A). As described for the Δ*pbdA* mutant, the inability of the Δ*pcaL* mutant to grow on the aromatic compounds was confirmed by monitoring CFU (Fig. S4). These data indicate that *p*-MBA and veratrate are catabolized through the β-ketoadipate pathway.

O-Demethylation of veratrate

Catabolism of veratrate through the protocatechuate arm of the β-ketoadipate pathway requires *O*-demethylations at its *para* and *meta* positions. To determine the order of the *para*- and *meta*-*O*-demethylation reactions catalyzed by PbdAB and VanAB, respectively, we grew the Δ*pbdA* and Δ*vanA* mutants to stationary phase in media supplemented with benzoate, and then we spiked in veratrate and monitored the metabolite profiles. Neither the Δ*pbdA* mutant nor the previously constructed Δ*vanA* mutant (40) exhibited additional growth on veratrate (Fig. 5). When veratrate was spiked into the growth medium of the Δ*pbdA* strain, isovanillate accumulated in the cell supernatant (Fig. 5B). Conversely, when veratrate was added to the Δ*vanA* strain, vanillate accumulated in the

TABLE 3 Description of RHA1 genes identified in this study

Gene	ORF[a]	Description	Closest characterized homolog	ID[b]	Ref
pbdA	RS14355	Cytochrome P450	CYP199A25, *Arthrobacter* sp.	74	(13)
pbdB	RS14360	PDR-type oxidoreductase	Phenoxybenzoate dioxygenase reductase PobB, *Pseudomonas pseudoalcaligenes* POB310	47	(53)
pbdR	RS14365	TetR/AcrR family transcriptional regulator	Tetracycline repressor protein, *Escherichia coli*	33	(54)
pobA	RS12415	*p*-hydroxybenzoate-3-hydroxylase	PHBH, *Rhodococcus opacus* 557	98	(55)

[a]In the ID of the open reading frame (ORF), the prefix "RHA1_" was dropped for simplicity.
[b]Percent amino acid sequence identity over entire length.

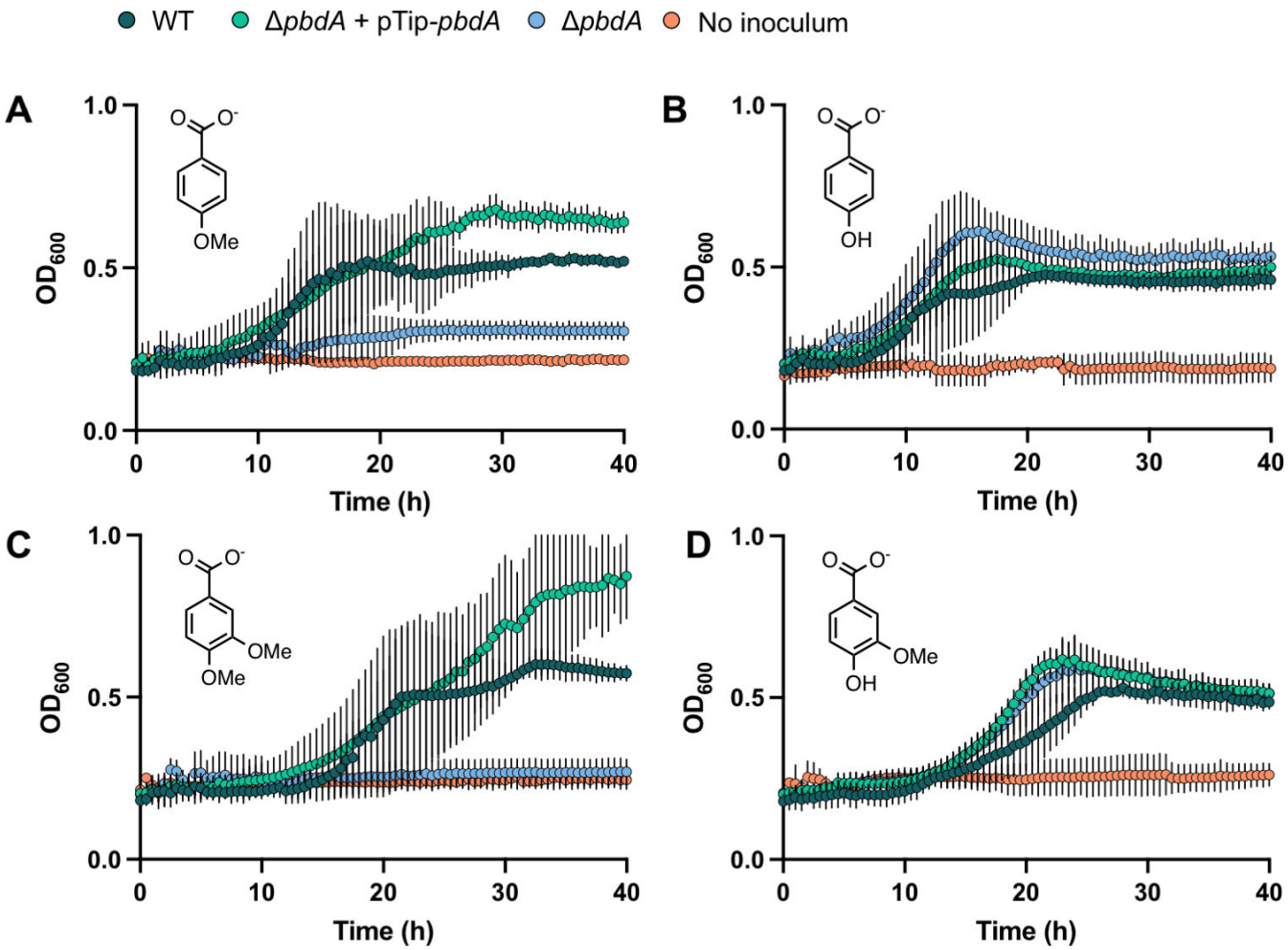

FIG 3 The role of *pbdA* in the growth of RHA1 on components of methylated lignin stream. Tested strains were wild-type (WT) RHA1, the Δ*pbdA* mutant, and its complement (Δ*pbdA* + pTip *pbdA*). Strains were grown in 96-well plates at 30°C on minimal medium supplemented with 5 mM (A) *p*-MBA, (B) veratrate, (C) *p*-HBA, or (D) vanillate. Data points represent the average of three biological replicates, and error bars represent the standard deviation.

cell supernatant (Fig. 5C). These results support the hypothesis that PbdA catalyzes the *p*-*O*-demethylation of veratrate and VanA catalyzes the *m*-*O*-demethylation of veratrate (Fig. 5D). Both appear to be highly specific, as the *p*-*O*-demethylated product was not detected for Δ*vanA* and the *m*-*O*-demethylated product was not detected for Δ*pbdA*. Moreover, both enzymes can tolerate a methoxy substituent *ortho* to the one being removed. However, only vanillate was transiently detected when veratrate was added to wild-type cells (Fig. 5A).

Identification and characterization of *pobA*

In many genera including *Rhodococcus*, the hydroxylation of *p*-HBA to protocatechuate is catalyzed by *para*-hydroxybenzoate-3-hydroxylase (PHBH), a flavin-containing oxygenase, also known as PobA (56). The RHA1 gene RS12415 encodes an enzyme that is predicted to be a PHBH (Table 3) (57). To investigate the role of this enzyme in *p*-MBA metabolism in RHA1, we constructed a Δ*pobA* deletion mutant. The mutant did not grow on *p*-HBA (Fig. 6) but grew on benzoate (Fig. S7). Complementation of the Δ*pobA* strain using an integration vector bearing *pobA* rescued growth (Fig. 6). These results indicate that PobA is necessary for catabolism of *p*-HBA, catalyzing its hydroxylation and the second step of *p*-MBA metabolism.

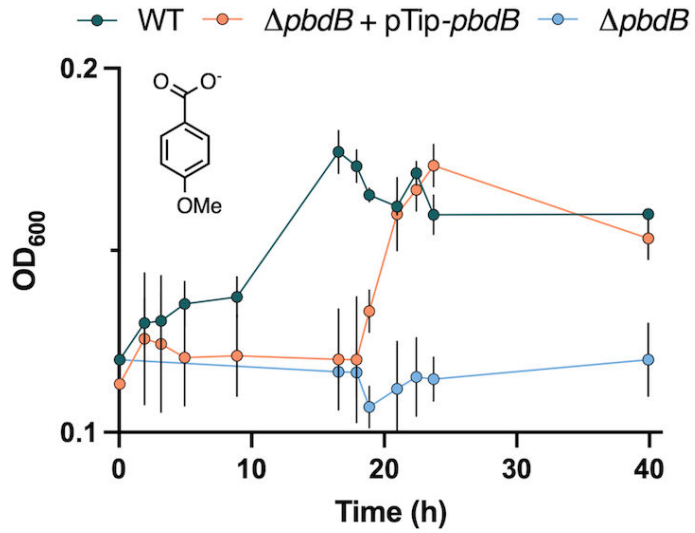

FIG 4 The role of *pbdB* in the growth of RHA1 on *p*-MBA. Wild type (WT), the Δ*pbdB* mutant, and its complement (Δ*pbdB* + pTip *pbdB*) were grown on 5 mM *p*-MBA in 48-well plates. Data points represent the average of three biological replicates, and error bars represent the standard deviation.

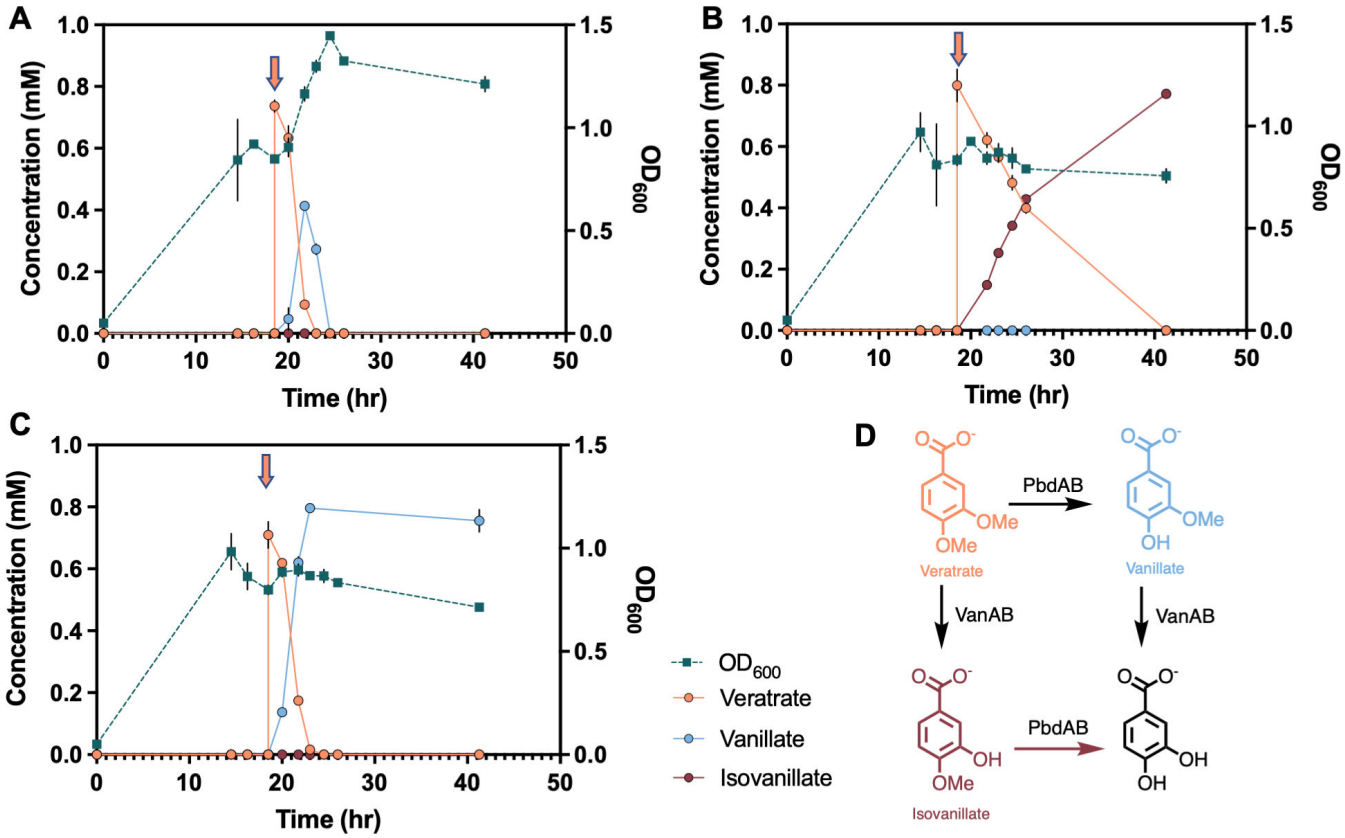

FIG 5 Metabolite accumulation in supernatants of RHA1 and mutants when supplemented with veratrate. Strains tested are wild-type (WT) RHA1 (A), the Δ*pbdA* mutant (B), and the Δ*vanA* mutant (C). Cultures were grown on 1 mM benzoate until apparent stationary phase, at which point (*t* = 18.5 h, indicated by the teal arrow), 0.8 mM veratrate was spiked into the media. (D) Putative metabolic pathway for degradation of veratrate in RHA1. Cultures were grown in 25 mL of culture in 125 mL flasks. Veratrate, vanillate, and isovanillate concentrations were measured using HPLC. Data points represent the mean of three biological replicates, and error bars indicate the standard deviation.

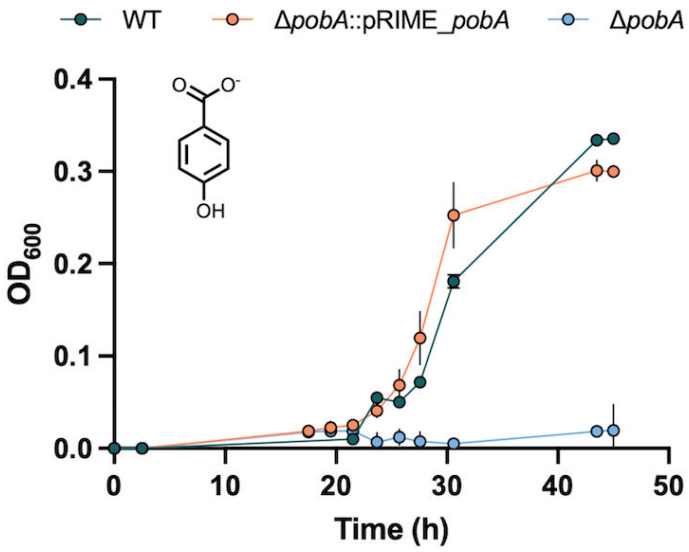

FIG 6 The role of *pobA* in the growth of RHA1 on *p*-HBA. Wild type (WT), the Δ*pobA* mutant, and its complement (Δ*pobA*::pRIME_*pobA*) were grown on 5 mM *p*-HBA in 48-well plates. Data points represent the average of three biological replicates, and error bars represent the standard deviation.

Growth of RHA1 on veratraldehyde and vanillin dehydrogenase activity

Because RHA1 completely consumed the veratraldehyde in the methylated lignin stream, we evaluated the growth of RHA1 on veratraldehyde. RHA1 grew robustly on veratraldehyde and, during this growth, transiently accumulated veratrate, isovanillate, and vanillate (Fig. 7A through C). We hypothesized that Vdh, the aromatic aldehyde dehydrogenase that transforms vanillin to vanillate, also oxidizes veratraldehyde. Consistent with this hypothesis, the previously constructed Δ*vdh* strain of RHA1 (40) did not grow on 2 mM veratraldehyde. Moreover, complementing the mutant with an integrated copy of *vdh* rescued growth after 90 h (Fig. 8). These results indicate that Vdh is necessary for veratraldehyde catabolism in RHA1.

Discussion

Using both pine and poplar substrates, Palumbo et al. recently developed a catalytic oxidation method to cleave the C–C bonds in lignin dimers and oligomers that had undergone methyl protection of the phenolic hydroxyl groups (7), thereby enabling aromatic monomer yields from lignin that exceed those accessible from C–O bond cleavage alone. Given the need for phenol stabilization in autoxidation catalysis, the output of this catalytic oxidation process is a slate of methylated aromatic compounds. In the present study, we showed that RHA1 grows on the oxidized pine lignin stream produced using the same approach, and that RHA1 efficiently catabolizes the three major aromatic monomers found in this stream—*p*-MBA, veratrate, and veratraldehyde—as well as acetate. Targeted gene deletion and metabolite analysis yielded a comprehensive metabolic network for veratraldehyde, veratrate, and *p*-MBA catabolism in RHA1 (Fig. 9). In this network, PbdAB catalyzes the *O*-demethylation of *p*-MBA to *p*-HBA, which is hydroxylated by PobA to form protocatechuate. Vdh, previously characterized as a vanillin dehydrogenase, also catalyzes the oxidation of veratraldehyde to veratrate. The VanAB RO and PbdAB P450 systems both catalyze the *O*-demethylation of veratrate at physiologically relevant rates, as revealed by measuring accumulation of metabolites. VanAB and PbdAB also catalyze the *O*-demethylation of vanillate and isovanillate, respectively, to protocatechuate. Thus, the catabolism of the three major aromatic monomers converges at protocatechuate, which feeds into central carbon metabolism via the β-ketoadipate pathway.

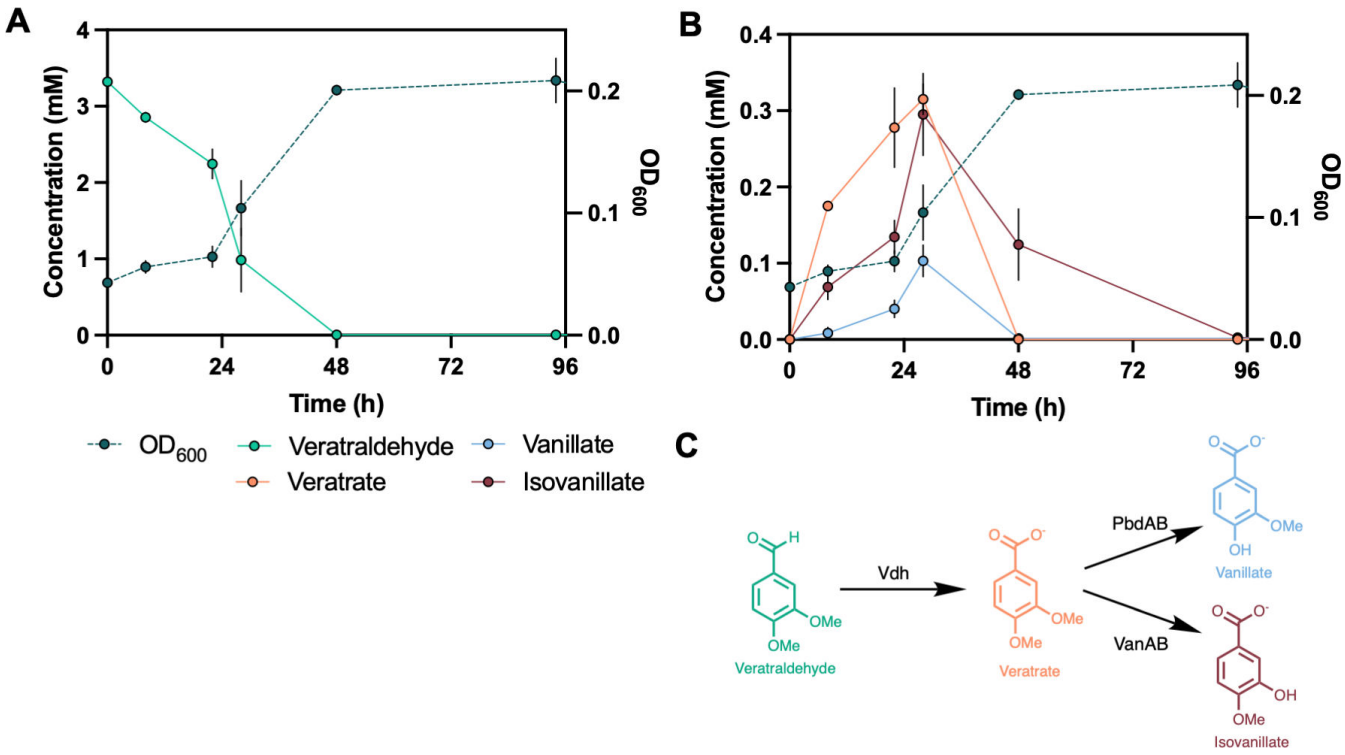

FIG 7 Growth of RHA1 on 3 mM veratraldehyde. (A) Depletion of veratraldehyde and (B) appearance of aromatic intermediates were monitored using HPLC. (C) Reaction scheme of the putative reactions generating detected intermediates. Cultures were grown in flasks on minimal medium supplemented with veratraldehyde at 30°C. Values represent the mean of biological triplicates, and error bars represent the standard deviation.

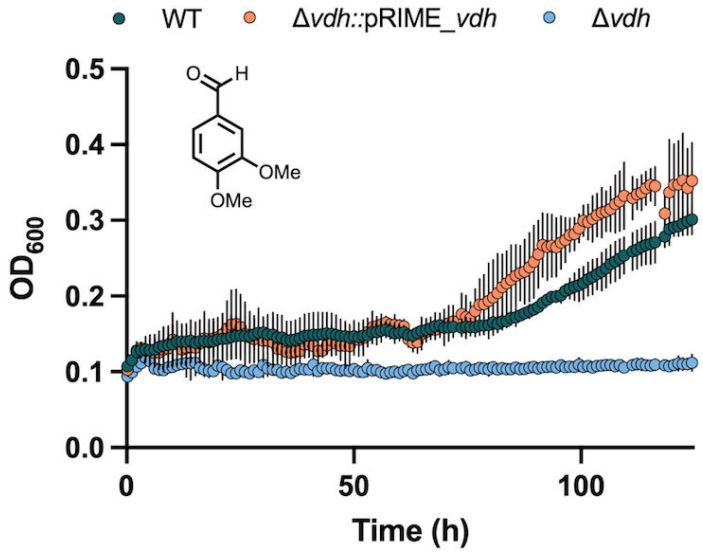

FIG 8 The role of *vdh* in the growth of RHA1 on veratraldehyde. Wild type (WT), the *vdh* mutant, and its complement (Δ*vdh*::pRIME_*vdh*) were grown on 5 mM veratraldehyde in 96-well plates. Data points represent the average of three biological replicates, and error bars represent the standard deviation.

The ability of VanA and PbdA to catalyze the respective *meta*- and *para*-*O*-demethylation of veratrate is consistent with the available biochemical studies of homologous enzymes. VanAB from *C. testosteroni* and *Streptomyces* sp. NL15-2K catalyzed the *meta*-*O*-demethylation of veratrate at 18% and 56% efficiency with respect to vanillate, respectively (9, 10). With respect to homologs of PbdA, CYP199A4 and CYP199A25 catalyze the

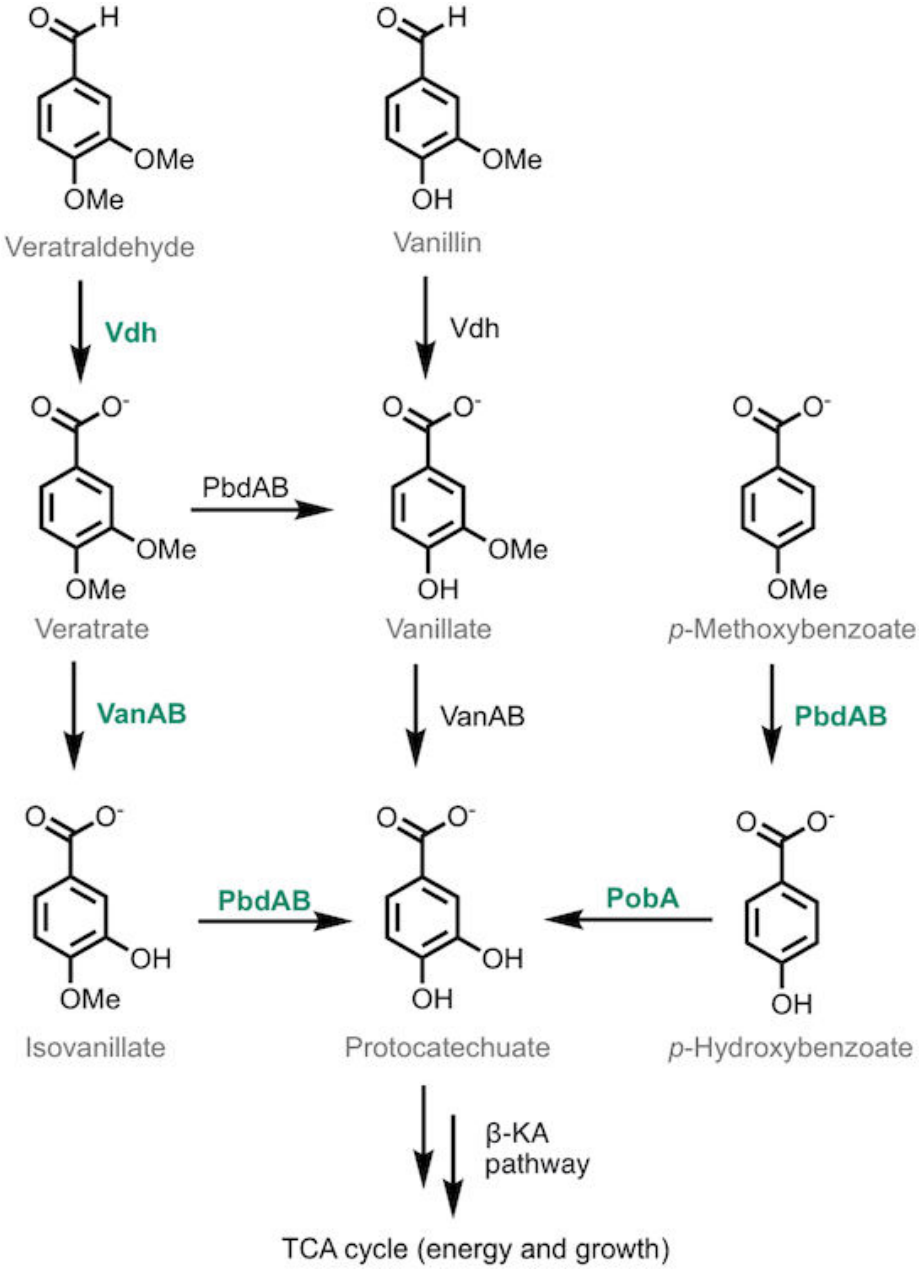

FIG 9 Proposed catabolism of veratraldehyde, veratrate, and *p*-methoxybenzoate in RHA1. Veratraldehyde and vanillin are oxidized to veratrate and vanillate, respectively. Veratraldehyde, vanillin, and *p*-MBA catabolism converge at protocatechuate, which is catabolized via the β-ketoadipate pathway (β-KA), which includes two successive reactions catalyzed by PcaL (Fig. S6). Green font denotes enzymatic steps validated in this study.

transformation of veratrate, although the closely related CYP199A2 apparently does not (13, 14). Specificity has only been reported for CYP199A4, which catalyzes the *p*-*O*-demethylation of veratrate at approximately 50% of the rate of *p*-MBA (14). Two observations suggest that *p*-*O*-demethylation is the preferred first step in the catabolism of veratrate. First, the Δ*vanA* strain accumulated vanillate faster than the Δ*pbdA* strain accumulated isovanillate (Fig. 5B and C). Second, only vanillate was detected during growth of wild-type RHA1 on veratrate (Fig. 5A). Interestingly, isovanillate and vanillate were detected at near-equivalent concentrations during growth on veratraldehyde. The reason for this is unclear, although transcriptomic studies of RHA1 grown on veratrate and veratraldehyde might illuminate whether this reflects an underlying regulatory

mechanism. Alternatively, the detected metabolites might reflect the substrate specificities of the respective *O*-demethylase systems. Recently, Palumbo et al. engineered *P. putida* KT2440 (KT2440) to convert veratrate and veratraldehyde from methylated lignin streams to muconate (7). As KT2440 has no native *p*-*O*-demethylase active on veratrate, the *p*-*O*-demethylase CYP199A4-HaPuR-HaPux system from *R. palustris* HaA2 was integrated into the genome. However, this strain accumulated isovanillate, arising from the VanAB-catalyzed *meta*-*O*-demethylation of veratrate. By contrast, incorporation of the *meta*-*O*-demethylase system from *C. testosteroni* strain BR6020, IvaAB, yielded a strain that did not accumulate isovanillate. These results indicate that the CYP199A4-HaPuR-HaPux system in an engineered biocatalyst has lower activity on isovanillate compared to the activity of the native PbdAB in RHA1. The lower activity of the system may be due to either enzyme specificity or differential expression.

The aromatic ring hydroxylation catalyzed by $PobA_{RHA1}$ can also be rate-limiting in the biotransformation of LDACs (22). For example, hydroxylation is a bottleneck in the biocatalytic transformation of *p*-HBA by KT2440 due to the specificity of the PHBH in this strain for NADPH (58, 59). By contrast, $PobA_{RHA1}$ is a member of the NADH-obligate PHBH clade (55). In the present work, *p*-HBA was not detected during growth of RHA1 on the methylated lignin stream. However, the concentration of substrate in these studies was relatively low. Therefore, it is possible that the hydroxylation of *p*-HBA might be rate-limiting under other conditions, particularly as other steps, such as *O*-demethylation, were optimized by strain engineering. Ultimately, further studies into the hydroxylation of *p*-HBA in RHA1 are required as it and related strains are developed as biocatalysts tailored to utilize *p*-HBA and its chemical precursors such as *p*-MBA and *p*-coumaric acid.

The involvement of Vdh, previously characterized for its activity on vanillin, in the dehydrogenation of veratraldehyde is consistent with biochemical studies of aromatic aldehyde dehydrogenases. More specifically, homologs of Vdh catalyze the dehydrogenation of veratraldehyde with up to 87% of the efficiency of vanillin (60–62). However, the enzymes characterized to date have broad specificity, and some have relatively low activity on veratraldehyde. Strikingly, RHA1 grew on concentrations of veratraldehyde up to 5 mM, which is much higher than the maximal concentration of 1 mM vanillin that RHA1 tolerates (40). It is unclear whether Vdh_{RHA1} contributes to this toxicity differential. In this respect, it would be insightful to determine the specificity of Vdh for the two compounds. Vanillin is a known antimicrobial agent, the mechanism of which has been attributed to aldehyde-induced DNA, protein damage, and membrane destabilization (63–65). Conversely, veratraldehyde toxicity is poorly described; it is possible that the higher tolerance of RHA1 for this compound reflects the different properties of the two chemicals.

The discovery and characterization of *O*-demethylation systems facilitate their optimization for the development of biocatalysts for lignin valorization. For example, as a two-component system, PbdAB may be advantageous for biocatalytic applications over the three-component CYP199A systems characterized to date. Moreover, characterizing the substrate range of VanAB and PbdAB, when complemented with structural and biochemical experiments, allows for rational engineering and optimization of these enzymes for biocatalysis. Indeed, previous studies on P450 demethylases have established that they are exceptionally amenable to engineering (50, 66–69). Similarly, new insights into RO structure and mechanism have revealed the engineering potential of these enzymes (70, 71). Such advances suggest the possibility of engineering enzymes like VanA and PbdA to transform the tri-methoxylated compounds generated from hardwood biomass fractionation with methyl protection (7, 72). More generally, elucidating the enzymes that catalyze the key reactions in catabolism of the aromatic monomers in methylated lignin streams expands the genetic and enzymatic toolkit for engineering novel biocatalysts. Furthermore, the robust and efficient catabolism of these compounds by RHA1 highlights the potential of rhodococcal biocatalysts for valorizing lignin.

ACKNOWLEDGMENTS

C.T.P. and G.T.B. thank the U.S. Department of Energy, Office of Energy Efficiency and Renewable Energy, Bioenergy Technologies Office for funding. A.C.B. and G.T.B. acknowledge support from The Center for Bioenergy Innovation, a U.S. Department of Energy Research Center supported by the Office of Biological and Environmental Research in the DOE Office of Science. The views expressed in the article do not necessarily represent the views of the DOE or the U.S. Government. The U.S. Government retains and the publisher, by accepting the article for publication, acknowledges that the U.S. Government retains a nonexclusive, paid-up, irrevocable, worldwide license to publish or reproduce the published form of this work, or allow others to do so, for U.S. Government purposes.

This study was supported by a grant from the Natural Sciences and Engineering Research Council of Canada (DG 171359). M.E.W. is the recipient of a Canada Graduate Scholarship-Doctoral. L.D.E. is the recipient of a Canada Research Chair. This work was authored in part by Alliance for Sustainable Energy, LLC, the manager and operator of the National Renewable Energy Laboratory for the U.S. Department of Energy (DOE) under Contract No. DE-AC36-08GO28308.

AUTHOR AFFILIATIONS

[1]Department of Microbiology and Immunology, Life Sciences Institute, The University of British Columbia, Vancouver, Canada
[2]Renewable Resources and Enabling Sciences Center, National Renewable Energy Laboratory, Golden, Colorado, USA

AUTHOR ORCIDs

Megan E. Wolf http://orcid.org/0000-0001-8236-8201
Gregg T. Beckham http://orcid.org/0000-0002-3480-212X
Lindsay D. Eltis http://orcid.org/0000-0002-6774-8158

FUNDING

Funder	Grant(s)	Author(s)
Canadian Government | Natural Sciences and Engineering Research Council of Canada (NSERC)	171359	Megan E. Wolf Anne T. Lalande Brianne L. Newman Lindsay D. Eltis
U.S. Department of Energy (DOE)	DE-AC36-08GO28308	Alissa C. Bleem Chad T. Palumbo Gregg T. Beckham
DOE | Office of Energy Efficiency and Renewable Energy (EERE)		Chad T. Palumbo Gregg T. Beckham
DOE | EERE | Office of Sustainable Transportation | Bioenergy Technologies Office (BETO)		Chad T. Palumbo Gregg T. Beckham

AUTHOR CONTRIBUTIONS

Megan E. Wolf, Formal analysis, Investigation, Writing – original draft, Writing – review and editing | Anne T. Lalande, Formal analysis, Investigation, Writing – review and editing | Brianne L. Newman, Investigation, Writing – review and editing | Alissa C. Bleem, Methodology, Writing – review and editing | Chad T. Palumbo, Formal analysis, Investigation, Writing – review and editing | Gregg T. Beckham, Funding acquisition, Writing –

review and editing | Lindsay D. Eltis, Conceptualization, Funding acquisition, Writing – original draft, Writing – review and editing

DATA AVAILABILITY

Additional data can be found in the supplemental material.

ADDITIONAL FILES

The following material is available online.

Supplemental Material

Fig. S1 to S8, Tables S1 and S2 (AEM02155-23-s0001.docx). Supplemental figures and tables.

REFERENCES

1. Boerjan W, Ralph J, Baucher M. 2003. Lignin biosynthesis. Annu Rev Plant Biol 54:519–546. https://doi.org/10.1146/annurev.arplant.54.031902.134938
2. del Río JC, Rencoret J, Gutiérrez A, Elder T, Kim H, Ralph J. 2020. Lignin monomers from beyond the canonical monolignol biosynthetic pathway: another brick in the wall. ACS Sustainable Chem Eng 8:4997–5012. https://doi.org/10.1021/acssuschemeng.0c01109
3. Rinaldi R, Jastrzebski R, Clough MT, Ralph J, Kennema M, Bruijnincx PCA, Weckhuysen BM. 2016. Paving the way for lignin valorisation: recent advances in bioengineering, biorefining and catalysis. Angew Chem Int Ed Engl 55:8164–8215. https://doi.org/10.1002/anie.201510351
4. Eltis L, Singh R. 2018. Chapter 11: biological funneling as a means of transforming lignin-derived aromatic compounds into value-added chemicals. RSC Energy Environ Ser:290–313. https://doi.org/10.1039/9781788010351
5. Beckham GT, Johnson CW, Karp EM, Salvachúa D, Vardon DR. 2016. Opportunities and challenges in biological lignin valorization. Curr Opin Biotechnol 42:40–53. https://doi.org/10.1016/j.copbio.2016.02.030
6. Weiland F, Kohlstedt M, Wittmann C. 2022. Guiding stars to the field of dreams: metabolically engineered pathways and microbial platforms for a sustainable lignin-based industry. Metab Eng 71:13–41. https://doi.org/10.1016/j.ymben.2021.11.011
7. Palumbo CT, Gu NX, Bleem AC, Sullivan KP, Katahira R, Stanley LM, Kenny JK, Ingraham MA, Ramirez KJ, Haugen SJ, Amendola CR, Stahl SS, Beckham GT. 2023. Catalytic carbon-carbon bond cleavage in lignin via manganese zirconium-mediated autoxidation. Nat Commun 15:862. https://doi.org/10.1038/s41467-024-45038-z
8. Buswell JA, Mahmood A. 1972. Bacterial degradation of *p*-methoxybenzoic acid. Arch Mikrobiol 84:275–286. https://doi.org/10.1007/BF00409077
9. Providenti MA, O'Brien JM, Ruff J, Cook AM, Lambert IB. 2006. Metabolism of isovanillate, vanillate, and veratrate by *Comamonas testosteroni* strain BR6020. J Bacteriol 188:3862–3869. https://doi.org/10.1128/JB.01675-05
10. Nishimura M, Nishimura Y, Abe C, Kohhata M. 2014. Expression and substrate range of *Streptomyces* vanillate demethylase. Biol Pharm Bull 37:1564–1568. https://doi.org/10.1248/bpb.b14-00337
11. Karlson U, Dwyer DF, Hooper SW, Moore ER, Timmis KN, Eltis LD. 1993. Two independently regulated cytochromes P-450 in a *Rhodococcus rhodochrous* strain that degrades 2-ethoxyphenol and 4-methoxybenzoate. J Bacteriol 175:1467–1474. https://doi.org/10.1128/jb.175.5.1467-1474.1993
12. Bell SG, Xu F, Forward I, Bartlam M, Rao Z, Wong LL. 2008. Crystal structure of CYP199A2, a para-substituted benzoic acid oxidizing cytochrome P450 from *Rhodopseudomonas palustris*. J Mol Biol 383:561–574. https://doi.org/10.1016/j.jmb.2008.08.033
13. Klenk JM, Ertl J, Rapp L, Fischer M-P, Hauer B. 2020. Expression and characterization of the benzoic acid hydroxylase CYP199A25 from *Arthrobacter* sp. Mol Cat 484:110739. https://doi.org/10.1016/j.mcat.2019.110739
14. Bell SG, Tan ABH, Johnson EOD, Wong LL. 2010. Selective oxidative demethylation of veratric acid to vanillic acid by CYP199A4 from *Rhodopseudomonas palustris* HaA2. Mol Biosyst 6:206–214. https://doi.org/10.1039/b913487e
15. Wu X, De bruyn M, Barta K. 2023. Deriving high value products from depolymerized lignin oil, aided by (bio)catalytic funneling strategies. Chem Commun 59:9929–9951. https://doi.org/10.1039/D3CC01555F
16. Sun Z, Fridrich B, de Santi A, Elangovan S, Barta K. 2018. Bright side of lignin depolymerization: toward new platform chemicals. Chem Rev 118:614–678. https://doi.org/10.1021/acs.chemrev.7b00588
17. Schutyser W, Renders T, Van den Bosch S, Koelewijn S-F, Beckham GT, Sels BF. 2018. Chemicals from lignin: an interplay of lignocellulose fractionation, depolymerisation, and upgrading. Chem Soc Rev 47:852–908. https://doi.org/10.1039/c7cs00566k
18. Liao Y, Koelewijn S-F, Van den Bossche G, Van Aelst J, Van den Bosch S, Renders T, Navare K, Nicolaï T, Van Aelst K, Maesen M, Matsushima H, Thevelein JM, Van Acker K, Lagrain B, Verboekend D, Sels BF. 2020. A sustainable wood biorefinery for low-carbon footprint chemicals production. Science 367:1385–1390. https://doi.org/10.1126/science.aau1567
19. Renders T, Van den Bosch S, Koelewijn S-F, Schutyser W, Sels BF. 2017. Lignin-first biomass fractionation: the advent of active stabilisation strategies. Energy Environ Sci 10:1551–1557. https://doi.org/10.1039/C7EE01298E
20. Subbotina E, Rukkijakan T, Marquez-Medina MD, Yu X, Johnsson M, Samec JSM. 2021. Oxidative cleavage of C-C bonds in lignin. Nat Chem 13:1118–1125. https://doi.org/10.1038/s41557-021-00783-2
21. Gu NX, Palumbo CT, Bleem AC, Sullivan KP, Haugen SJ, Woodworth SP, Ramirez KJ, Kenny JK, Stanley LD, Katahira R, Stahl SS, Beckham GT. 2023. Autoxidation catalysis for carbon–carbon bond cleavage in lignin. ACS Cent Sci 9:2277–2285. https://doi.org/10.1021/acscentsci.3c00813
22. Erickson E, Bleem A, Kuatsjah E, Werner AZ, DuBois JL, McGeehan JE, Eltis LD, Beckham GT. 2022. Critical enzyme reactions in aromatic catabolism for microbial lignin conversion. Nat Catal 5:86–98. https://doi.org/10.1038/s41929-022-00747-w
23. Li S, Du L, Bernhardt R. 2020. Redox partners: ffunction modulators of bacterial P450 enzymes. Trends Microbiol 28:445–454. https://doi.org/10.1016/j.tim.2020.02.012
24. Correll CC, Batie CJ, Ballou DP, Ludwig ML. 1992. Phthalate dioxygenase reductase - a modular structure for electron-transfer from pyridine-nucleotides to [2Fe-2S]. Science 258:1604–1610. https://doi.org/10.1126/science.1280857
25. Lanfranchi E, Trajković M, Barta K, de Vries JG, Janssen DB. 2019. Exploring the selective demethylation of aryl methyl ethers with a *Pseudomonas* rieske monooxygenase. Chembiochem 20:118–125. https://doi.org/10.1002/cbic.201800594
26. Zhang S-T, Li T, Deng S-K, Spain JC, Zhou N-Y. 2023. A cytochrome P450 system initiates 4-nitroanisole degradation in *Rhodococcus* sp. strain JS3073. J Hazard Mater 458:131886. https://doi.org/10.1016/j.jhazmat.2023.131886

27. Larkin MJ, Kulakov LA, Allen CCR. 2005. Biodegradation and *Rhodococcus* – masters of catabolic versatility. Curr Opin Biotechnol 16:282–290. https://doi.org/10.1016/j.copbio.2005.04.007
28. van der Geize R, Dijkhuizen L. 2004. Harnessing the catabolic diversity of rhodococci for environmental and biotechnological applications. Curr Opin Microbiol 7:255–261. https://doi.org/10.1016/j.mib.2004.04.001
29. Dexter GN, Navas LE, Grigg JC, Bajwa H, Levy-Booth DJ, Liu J, Louie NA, Nasseri SA, Jang S-K, Renneckar S, Eltis LD, Mohn WW. 2022. Bacterial catabolism of acetovanillone, a lignin-derived compound. Proc Natl Acad Sci U S A 119:e2213450119. https://doi.org/10.1073/pnas.2213450119
30. Levy-Booth DJ, Fetherolf MM, Stewart GR, Liu J, Eltis LD, Mohn WW. 2019. Catabolism of alkylphenols in *Rhodococcus* via a meta-cleavage pathway associated with genomic islands. Front Microbiol 10:1862. https://doi.org/10.3389/fmicb.2019.01862
31. Zhu Y, Liao Y, Lv W, Liu J, Song X, Chen L, Wang C, Sels BF, Ma L. 2020. Complementing vanillin and cellulose production by oxidation of lignocellulose with stirring control. ACS Sustainable Chem Eng 8:2361–2374. https://doi.org/10.1021/acssuschemeng.9b04837
32. Alherech M, Omolabake S, Holland CM, Klinger GE, Hegg EL, Stahl SS. 2021. From lignin to valuable aromatic chemicals: lignin depolymerization and monomer separation via centrifugal partition chromatography. ACS Cent Sci 7:1831–1837. https://doi.org/10.1021/acscentsci.1c00729
33. Cappelletti M, Presentato A, Piacenza E, Firrincieli A, Turner RJ, Zannoni D. 2020. Biotechnology of *Rhodococcus* for the production of valuable compounds. Appl Microbiol Biotechnol 104:8567–8594. https://doi.org/10.1007/s00253-020-10861-z
34. Gröger H, Asano Y, Bornscheuer UT, Ogawa J. 2012. Development of biocatalytic processes in Japan and Germany: from research synergies to industrial applications. Chem Asian J 7:1138–1153. https://doi.org/10.1002/asia.201200105
35. Frederick J, Hennessy F, Horn U, de la Torre Cortés P, van den Broek M, Strych U, Willson R, Hefer CA, Daran J-MG, Sewell T, Otten LG, Brady D. 2020. The complete genome sequence of the nitrile biocatalyst *Rhodocccus rhodochrous* ATCC BAA-870. BMC Genomics 21:3. https://doi.org/10.1186/s12864-019-6405-7
36. Jiao S, Li F, Yu H, Shen Z. 2020. Advances in acrylamide bioproduction catalyzed with *Rhodococcus* cells harboring nitrile hydratase. Appl Microbiol Biotechnol 104:1001–1012. https://doi.org/10.1007/s00253-019-10284-5
37. Liang Y, Jiao S, Wang M, Yu H, Shen Z. 2020. A CRISPR/Cas9-based genome editing system for *Rhodococcus ruber* TH. Metab Eng 57:13–22. https://doi.org/10.1016/j.ymben.2019.10.003
38. McLeod MP, Warren RL, Hsiao WWL, Araki N, Myhre M, Fernandes C, Miyazawa D, Wong W, Lillquist AL, Wang D, et al. 2006. The complete genome of *Rhodococcus* sp. RHA1 provides insights into a catabolic powerhouse. Proc Natl Acad Sci U S A 103:15582–15587. https://doi.org/10.1073/pnas.0607048103
39. Seto M, Kimbara K, Shimura M, Hatta T, Fukuda M, Yano K. 1995. A novel transformation of polychlorinated-biphenyls by *Rhodococcus* sp strain RHA1. Appl Environ Microbiol 61:3353–3358. https://doi.org/10.1128/aem.61.9.3353-3358.1995
40. Chen HP, Chow M, Liu CC, Lau A, Liu J, Eltis LD. 2012. Vanillin catabolism in *Rhodococcus jostii* RHA1. Appl Environ Microbiol 78:586–588. https://doi.org/10.1128/AEM.06876-11
41. Fetherolf MM, Levy-Booth DJ, Navas LE, Liu J, Grigg JC, Wilson A, Katahira R, Beckham GT, Mohn WW, Eltis LD. 2020. Characterization of alkylguaiacol-degrading cytochromes P450 for the biocatalytic valorization of lignin. Proc Natl Acad Sci U S A 117:25771–25778. https://doi.org/10.1073/pnas.1916349117
42. Patrauchan MA, Florizone C, Dosanjh M, Mohn WW, Davies J, Eltis LD. 2005. Catabolism of benzoate and phthalate in *Rhodococcus* sp. strain RHA1: redundancies and convergence. J Bacteriol 187:4050–4063. https://doi.org/10.1128/JB.187.12.4050-4063.2005
43. Harazono K, Yamashita N, Shinzato N, Watanabe Y, Fukatsu T, Kurane R. 2003. Isolation and characterization of aromatics-degrading microorganisms from the gut of the lower termite *Coptotermes formosanus*. Biosci Biotechnol Biochem 67:889–892. https://doi.org/10.1271/bbb.67.889
44. Paliwal V, Raju SC, Modak A, Phale PS, Purohit HJ. 2014. *Pseudomonas putida* CSV86: a candidate genome for genetic bioaugmentation. PLoS One 9:e84000. https://doi.org/10.1371/journal.pone.0084000
45. Jang JH, Brandner DG, Dreiling RJ, Ringsby AJ, Bussard JR, Stanley LM, Happs RM, Kovvali AS, Cutler JI, Renders T, Bielenberg JR, Román-Leshkov Y, Beckham GT. 2022. Multi-pass flow-through reductive catalytic fractionation. Joule 6:1859–1875. https://doi.org/10.1016/j.joule.2022.06.016
46. Vaillancourt FH, Han S, Fortin PD, Bolin JT, Eltis LD. 1998. Molecular basis for the stabilization and inhibition of 2, 3-dihydroxybiphenyl 1, 2-dioxygenase by t-butanol. J Biol Chem 273:34887–34895. https://doi.org/10.1074/jbc.273.52.34887
47. Russell DW, Sambrook J. 2001. Molecular cloning: a laboratory manual. vol 1. Cold Spring Harbor Laboratory, Cold Spring Harbor, NY.
48. van der Geize R, Hessels GI, van Gerwen R, van der Meijden P, Dijkhuizen L. 2001. Unmarked gene deletion mutagenesis of *kstD*, encoding 3-ketosteroid Δ^1-dehydrogenase, in *Rhodococcus erythropolis* SQ1 using *sacB* as counter-selectable marker. FEMS Microbiol Lett 205:197–202. https://doi.org/10.1111/j.1574-6968.2001.tb10947.x
49. Round JW, Robeck LD, Eltis LD. 2021. An integrative toolbox for synthetic biology in *Rhodococcus*. ACS Synth Biol 10:2383–2395. https://doi.org/10.1021/acssynbio.1c00292
50. Mallinson SJB, Machovina MM, Silveira RL, Garcia-Borràs M, Gallup N, Johnson CW, Allen MD, Skaf MS, Crowley MF, Neidle EL, Houk KN, Beckham GT, DuBois JL, McGeehan JE. 2018. A promiscuous cytochrome P450 aromatic O-demethylase for lignin bioconversion. Nat Commun 9:2487. https://doi.org/10.1038/s41467-018-04878-2
51. Furuya T, Kino K. 2009. Discovery of 2-naphthoic acid monooxygenases by genome mining and their use as biocatalysts. ChemSusChem 2:645–649. https://doi.org/10.1002/cssc.200900054
52. Hinrichs W, Kisker C, Düvel M, Müller A, Tovar K, Hillen W, Saenger W. 1994. Structure of the Tet repressor-tetracycline complex and regulation of antibiotic resistance. Science 264:418–420. https://doi.org/10.1126/science.8153629
53. Dehmel U, Engesser K-H, Timmis KN, Dwyer DF. 1995. Cloning, nucleotide sequence, and expression of the gene encoding a novel dioxygenase involved in metabolism of carboxydiphenyl ethers in *Pseudomonas pseudoalcaligenes* POB310. Arch Microbiol 163:35–41. https://doi.org/10.1007/BF00262201
54. Postle K, Nguyen TT, Bertrand KP. 1984. Nucleotide sequence of the repressor gene of the TN10 tetracycline resistance determinant. Nucleic Acids Res 12:4849–4863. https://doi.org/10.1093/nar/12.12.4849
55. Jadan AP, Moonen MJH, Boeren S, Golovleva LA, Rietjens I, Berkel WJH. 2004. Biocatalytic potential of *p* - hydroxybenzoate hydroxylase from *Rhodococcus rhodnii* 135 and *Rhodococcus opacus* 557. Adv Synth Catal 346:367–375. https://doi.org/10.1002/adsc.200303146
56. Husain M, Massey V. 1979. Kinetic studies on the reaction of *p*-hydroxybenzoate hydroxylase. J Biol Chem 254:6657–6666. https://doi.org/10.1016/S0021-9258(18)50419-1
57. Westphal AH, Tischler D, Heinke F, Hofmann S, Gröning JAD, Labudde D, van Berkel WJH. 2018. Pyridine nucleotide coenzyme specificity of *p*-hydroxybenzoate hydroxylase and related flavoprotein monooxygenases. Front Microbiol 9:3050. https://doi.org/10.3389/fmicb.2018.03050
58. Kuatsjah E, Johnson CW, Salvachúa D, Werner AZ, Zahn M, Szostkiewicz CJ, Singer CA, Dominick G, Okekeogbu I, Haugen SJ, Woodworth SP, Ramirez KJ, Giannone RJ, Hettich RL, McGeehan JE, Beckham GT. 2022. Debottlenecking 4-hydroxybenzoate hydroxylation in *Pseudomonas putida* KT2440 improves muconate productivity from *p*-coumarate. Metab Eng 70:31–42. https://doi.org/10.1016/j.ymben.2021.12.010
59. Salvachúa D, Johnson CW, Singer CA, Rohrer H, Peterson DJ, Black BA, Knapp A, Beckham GT. 2018. Bioprocess development for muconic acid production from aromatic compounds and lignin. Green Chem 20:5007–5019. https://doi.org/10.1039/C8GC02519C
60. Nishimura M, Kawakami S, Otsuka H. 2018. Molecular cloning and characterization of vanillin dehydrogenase from *Streptomyces* sp. NI15-2K. BMC Microbiol 18:154. https://doi.org/10.1186/s12866-018-1309-2
61. Kamimura N, Goto T, Takahashi K, Kasai D, Otsuka Y, Nakamura M, Katayama Y, Fukuda M, Masai E. 2017. A bacterial aromatic aldehyde dehydrogenase critical for the efficient catabolism of syringaldehyde. Sci Rep 7:44422. https://doi.org/10.1038/srep44422

62. Masai E, Yamamoto Y, Inoue T, Takamura K, Hara H, Kasai D, Katayama Y, Fukuda M. 2007. Characterization of *ligV* essential for catabolism of vanillin by *Sphingomonas paucimobilis* SYK-6. Biosci Biotechnol Biochem 71:2487–2492. https://doi.org/10.1271/bbb.70267
63. Fitzgerald DJ, Stratford M, Gasson MJ, Ueckert J, Bos A, Narbad A. 2004. Mode of antimicrobial action of vanillin against *Escherichia coli, Lactobacillus plantarum* and *Listeria innocua*. J Appl Microbiol 97:104–113. https://doi.org/10.1111/j.1365-2672.2004.02275.x
64. LoPachin RM, Gavin T. 2014. Molecular mechanisms of aldehyde toxicity: a chemical perspective. Chem Res Toxicol 27:1081–1091. https://doi.org/10.1021/tx5001046
65. Simon O, Klaiber I, Huber A, Pfannstiel J. 2014. Comprehensive proteome analysis of the response of *Pseudomonas putida* KT2440 to the flavor compound vanillin. J Proteomics 109:212–227. https://doi.org/10.1016/j.jprot.2014.07.006
66. Bell SG, Zhou R, Yang W, Tan ABH, Gentleman AS, Wong L-L, Zhou W. 2012. Investigation of the substrate range of CYP199A4: modification of the partition between hydroxylation and desaturation activities by substrate and protein engineering. Chemistry 18:16677–16688. https://doi.org/10.1002/chem.201202776
67. Ellis ES, Hinchen DJ, Bleem A, Bu L, Mallinson SJB, Allen MD, Streit BR, Machovina MM, Doolin QV, Michener WE, Johnson CW, Knott BC, Beckham GT, McGeehan JE, DuBois JL. 2021. Engineering a cytochrome P450 for demethylation of lignin-derived aromatic aldehydes. JACS Au 1:252–261. https://doi.org/10.1021/jacsau.0c00103
68. Machovina MM, Mallinson SJB, Knott BC, Meyers AW, Garcia-Borràs M, Bu L, Gado JE, Oliver A, Schmidt GP, Hinchen DJ, Crowley MF, Johnson CW, Neidle EL, Payne CM, Houk KN, Beckham GT, McGeehan JE, DuBois JL. 2019. Enabling microbial syringol conversion through structure-guided protein engineering. Proc Natl Acad Sci U S A 116:13970–13976. https://doi.org/10.1073/pnas.1820001116
69. Miller JC, Lee JHZ, Mclean MA, Chao RR, Stone ISJ, Pukala TL, Bruning JB, De Voss JJ, Schuler MA, Sligar SG, Bell SG. 2023. Engineering C–C bond cleavage activity into a P450 monooxygenase enzyme. J Am Chem Soc 145:9207–9222. https://doi.org/10.1021/jacs.3c01456
70. Brimberry M, Garcia AA, Liu J, Tian J, Bridwell-Rabb J. 2023. Engineering rieske oxygenase activity one piece at a time. Curr Opin Chem Biol 72:102227. https://doi.org/10.1016/j.cbpa.2022.102227
71. Tian J, Garcia AA, Donnan PH, Bridwell-Rabb J. 2023. Leveraging a structural blueprint to rationally engineer the rieske oxygenase TsaM. Biochemistry 62:1807–1822. https://doi.org/10.1021/acs.biochem.3c00150
72. Notonier S, Werner AZ, Kuatsjah E, Dumalo L, Abraham PE, Hatmaker EA, Hoyt CB, Amore A, Ramirez KJ, Woodworth SP, Klingeman DM, Giannone RJ, Guss AM, Hettich RL, Eltis LD, Johnson CW, Beckham GT. 2021. Metabolism of syringyl lignin-derived compounds in *Pseudomonas putida* enables convergent production of 2-pyrone-4,6-dicarboxylic acid. Metab Eng 65:111–122. https://doi.org/10.1016/j.ymben.2021.02.005